

Received: 2009.01.04
Accepted: 2009.01.27

CT diagnosis of early stroke – the initial approach to the new CAD tool based on multiscale estimation of ischemia

Jerzy Walecki¹, Artur Przelaskowski², Katarzyna Sklinda¹, Grzegorz Ostrek², Tomasz Bulski¹

¹ Department of Radiology, Medical Centre of Postgraduate Education, CSK, Warsaw, Poland

² Institute of Radioelectronics, Warsaw University of Technology, Warsaw, Poland

Author's address: Artur Przelaskowski, Institute of Radioelectronics, Warsaw University of Technology, Nowowiejska 15/19, Warsaw, Poland, e-mail: arturp@ire.pw.edu.pl

Source of support: Research supported by a scientific (2007–2009) N518 042 32/3301 grant from Ministry of Science and Higher Education, Poland

Summary

Background:

Computer aided diagnosis (CAD) becomes one of the most important diagnostic tools for urgent states in cerebral stroke and other life-threatening conditions where time plays a crucial role. Routine CT is still diagnostically insufficient in hyperacute stage of stroke that is in the therapeutic window for thrombolytic therapy. Authors present computer assistant of early ischemic stroke diagnosis that supports the radiologic interpretations. A new semantic-visualization system of ischemic symptoms applied to noncontrast, routine CT examination was based on multiscale image processing and diagnostic content estimation.

Material/Methods:

Evaluation of 95 sets of examinations in patients admitted to a hospital with symptoms suggesting stroke was undertaken by four radiologists from two medical centers unaware of the final clinical findings. All of the consecutive cases were considered as having no CT direct signs of hyperacute ischemia. At the first test stage only the CTs performed at the admission were evaluated independently by radiologists. Next, the same early scans were evaluated again with additional use of multiscale computer-assistant of stroke (MulCAS). Computerized suggestion with increased sensitivity to the subtle image manifestations of cerebral ischemia was constructed as additional view representing estimated diagnostic content with enhanced stroke symptoms synchronized to routine CT data preview. Follow-up CT examinations and clinical features confirmed or excluded the diagnosis of stroke constituting 'gold standard' to verify stroke detection performance.

Results:

Higher AUC (area under curve) values were found for MulCAS -aided radiological diagnosis for all readers and the differences were statistically significant for random readers-random cases parametric and non-parametric DBM MRMC analysis. Sensitivity and specificity of acute stroke detection for the readers was increased by 30% and 4%, respectively.

Conclusions:

Routine CT completed with proposed method of computer assisted diagnosis provided noticeable better diagnosis efficiency of acute stroke according to the rates and opinions of all test readers. Further research includes fully automatic detection of hypodense regions to complete assisted indications and formulate the suggestions of stroke cases more objectively. Planned prospective studies will let evaluate more accurately the impact of this CAD tool on diagnosis and further treatment in patients suffered from stroke. It is necessary to determine whether this method is possible to be applied widely.

Key words:

hyperacute stroke • CT • multiscale processing • computer aided diagnosis

PDF file:

<http://www.polradiol.com/fulltxt.php?ICID=879259>

Background

According to WHO definition stroke is the clinical syndrome of rapid onset of focal, or sometimes global, cerebral deficit with a vascular cause, lasting more than 24 hours or leading to death. Infarction may affect any area of the brain following vascular territory or watershed distribution. It is the leading cause of disability and one of the leading causes of mortality [1]. Brain imaging is required to classify stroke patients to acute interventions (thrombolysis), which is very important for stroke emergency centers. The clinical diagnosis of acute stroke is sometimes difficult and thus the role of neuroimaging is gaining significance. It should allow identification of patients with hyperacute infarctions and selection of treatment, exclusion of intracerebral hemorrhage and determination of etiology as well as follow-up therapy and its possible complications. Although MRI has an established and recently expanding role in diagnosis of early stroke, the difficulties with getting access to this examination often require the use of CT [2]. Consequently, CT is widely used and considered as the method of first choice for differentiating the stroke syndrome. Such imaging of acute stroke pathology allows the early assessment of irreversible ischemic injury. Although a CT image of the brain in acute stroke patients is not difficult to read, it is rather not self-evident. Reading of CT needs training and instructions, how to recognize anatomy and pathology, combined with knowledge about the physical conditions of image contrast [3].

The recent advent of thrombolytic therapy for hyperacute stroke treatment makes the earliest detection of areas of hypoattenuating ischemic parenchyma exceedingly important [3–5]. Accurate early diagnosis of hyperacute infarctions is critical due to limited timing of thrombolytic therapy. However in hyperacute stage of ischemic stroke (0–6 h), in most cases, we observe normal brain tissue in CT studies and a focal hypodense area as direct sign of pathology is imperceptible. Sometimes, early indirect findings, like obscuration of gray/white matter differentiation and effacement of sulci or loss of insular ribbon sign may be noticed instead. Poorly defined regions of lower density ischemia becoming more sharply delineated in the following hours. Thus, it becomes possible to notice a slight hypodense area of infarction either in the cortices or the basal ganglia [5–6]. However, many infarcts do not emerge on CT even until many hours after the onset of stroke – 50/60% of stroke cases have normal CT before 12 h after stroke onset [7]. Hence, reliable computer assistance with accurate and convincing indications of stroke was considered to improve diagnostic value of CT examinations for those cases.

Generally, computer aided diagnosis (CAD) has become one of the major research subjects in medical imaging and diagnostic radiology [8]. CAD is defined as a diagnosis that is made by a radiologist who uses the output from a computerized understanding of medical images as an assistance or "second opinion" in detecting lesions and in making diagnostic decisions; the final diagnosis is made by the radiologist [9]. Effective methods of CAD are based on the fundamental content modeling concepts taking into consideration the following key issues:

- a) computational image descriptors: flexible, reliable and specific numerical description of diagnostic image content;
- b) more-less formalized medical knowledge: characteristics of human observers, taxonomy and complete ontology;
- c) semantic image understanding: methods of image processing, analysis and synthesis, pattern recognition and understanding adjusted to hierarchical and flexible cognitive resonance based on computational image descriptors and formalized medical knowledge;
- d) integration of medical imaging systems with advanced interfaces of diagnostic workstations and aiding tools [10].

CT imaging of acute stroke

Broad clinical criteria based on symptoms at presentation resulted in the enrollment of many patients, many of who ultimately were not diagnosed as having stroke. Apart from signs and symptoms, also changeable and unchangeable risk factors of stroke were taken into consideration on presentation [11]. Lately, perfusion CT has proved to be beneficial in the evaluation of acute stroke patients as it allows for fast qualitative and quantitative assessment of cerebral perfusion by generating maps of CBF, cerebral blood volume (CBV), mean transit time (MTT) and time-to-peak (TTP) [12]. Moreover, other modalities like SPECT and even ultrasonic transcranial harmonic imaging should be mentioned as possibly useful in certain cases of acute stroke diagnosis and therapy [13,14].

Due to its availability and regardless of the fact that many infarcts do not emerge on CT until hours after the onset of stroke, possibly the earliest CT maintains a principal position in the evaluation of patients with acute stroke. The majority of larger infarcts reveal within 6 h with typical sign of acute ischemia on CT-hypoattenuating zone within a defined arterial supply territory corresponding to irreversibly damaged brain tissue. Edema (which occurs initially) in the ischemic cortex reduces its contrast with respect to the adjacent white matter and provokes a loss of anatomic margins. Early CT findings in acute middle cerebral artery (MCA) infarction are obscuration of lentiform nucleus [15] which is due to cellular edema in the basal ganglia and a hyperattenuating MCA representing acute thrombus within the M1 segment as well as loss of the gray/white interface at the lateral margin of the insula, and called it the "loss of insular ribbon" sign described by Truwit et al. [16]. In the next stage, lasting for several days and up to 2 weeks so called "fogging" phenomenon occurs – infarcted zone becomes isodense and the extent of an infarction may be underestimated on CT. Then, by 2–3 months, the infarctions are easily visible as areas of water density [17].

According to standard templates, the site of the infarct is defined as subcortical, when internal border zone or deep arterial branch areas are involved, with additional differentiation between nonlacunar and lacunar infarcts. The latter is defined as a subcortical sharply delineated focal lesion with a diameter equal or less than 15 mm. Cortical infarct occurs, when superficial arterial branch territories are involved; cortico-subcortical, when concomitant involvement of arterial deep and superficial territories is present. The size of the infarct is quantified as follows –

small, when the lesion involves less than one half a lobe (or in some studies when CT scans are permanently negative); medium, when the lesion involves one half to one lobe; and large, when the lesion involves more than one lobe. Mass effect is defined as slight, when only a compression of ventricles without dislocation is present; moderate, when a partial ventricular shift across the midline is observed; and severe, when a total ventricular shift across the midline is described. The age of the lesion, and hence its relevance to the present clinical symptoms, is usually judged from the degree of the mass effect, the clarity of its margins, the degree of hypodensity and presence of hemorrhagic transformation.

Focal hypodense changes were found to be the most frequent and reliable signs of acute cerebral ischemia in CT imaging. A decline in cerebral blood flow causes the brain tissue to take up water immediately. Thus, in the early stage of cerebral ischemia, the tissue changes consist mainly in alteration of water and electrolyte content. Parallel intracellular increase of sodium and a decrease of potassium concentration occur. A 2–4% increase in brain tissue water within 4 h of MCA occlusion was noticed in several experiments [3,18]. Increase of water content causes the lowering of brain attenuation coefficients in hyperacute ischemia, which leads to a discrepant decrease of about 1.3–2.6 HU (Hounsfield Units) for 1% change in water content. Approximately 2–10 HU of CT attenuation decrease within 4h of MCA occlusion is rather not very high. The discrepancy of water uptake and density changes might suggest an incompleteness of ischemic physiology model and unclear impact of other factors, e.g. decreased lipids, increased protein and electrolyte changes. More generally, early ischemic changes may vary within the limited range of HU scale depending on cerebral infarct case, discrepant patient characteristics and acquisition conditioning. The attenuation coefficients of brain parenchyma vary, mainly due to the differing thickness of the cranial vault. Dense bone lowers the energy of the beam and increases attenuation. Bone, beam hardening artifacts as inter-individual density differences of up to 14 HU were noticed in brain parenchyma at comparable scan levels [19]. Additionally, the accuracy, stability and linearity of CT number (HU) and degradation of local contrast resolution are caused by noise (standard deviation up to 4HU) and CT number fluctuations of zero for water (within 2HU) because of variations in the stability of the detector system, x-ray source, non-optimum scanning and image reconstruction imperfectness. Such CT number instability masks subtle hypodense changes within ischemic region making pathology detection extremely difficult for many cases of irreversible infarcts.

Challenges and answers for acute stroke CADs

To sum up, the early hypodense changes are subtle, and ischemic area is not well outlined or contrasted. Slight changes in grey shade can hardly be distinguished in noisy and distorted areas because of a low brightness contrast. Because of the human eye limitations and medical imaging imperfectness, these first ischemic signs can often be out of sensitivity threshold. Thus, a challenge of CAD tool application is making hypodensity distribution more distinct to

reveal the diagnostic content and improve accurate recognition of infarct signatures.

Computer-aided acute stroke diagnosis was mostly based on unenhanced CT examinations [19–21] according to concept of sensing technologies with semantic image understanding. Sensing technologies are aimed at extracting information from events that are beyond the reach of human sensory ability. Desired effects of image post-processing are:

- a) noise suppression;
- b) omission or reduction of the content masking caused by image artifacts and other scanning conditioning;
- c) the enhancement of local mean density differentiation in segmented regions susceptible to stroke.

Besides approved methods of texture, shape and margins analysis applied in source image domain, multiscale methods of medical image analysis were found to be effective for many diagnosis-support applications [22]. Hierarchical and flexible multiresolution image representation is extremely useful for nonlinear image approximation and subtle or hidden signal extraction [23–5] because its capability for signal energy packing with controlled localization across spatial, scale and subband coordinates. Selection of proper transform basis allow specific target content modeling and modifying or extraction through adaptive thresholding.

Our research was directed to design, implementation and experimental evaluation of CAD method to improve acute stroke diagnosis based on extremely difficult cases of emergency CT scans. The most required effect of enhanced visibility of hidden hypodense signs, included additionally in scan review procedure, was increased ability to detect the hypodense area of hyperacute ischemic brain parenchyma.

Material and Methods

Preliminary tests and optimization procedures were performed to maximize hypodense signs extraction according to clearly defined diagnostic performance criteria. Such criteria were clarified through discussions of integrated team of neurologists, radiologists and engineers. Different quality datasets of stroke CT images from five scanners, and various cases of pathology were considered. Suspected location of ischemic hyperacute changes were determined according to follow-up data. Wavelet-based image processing methods was selected to enhance hypodense regions according to the following concept: – the initial gray-to-white tissue segmentation; – the next segmentation of possibly ischemic areas; – noise suppression in selected ROIs through the non-perfect signal reconstruction in successive scales, basing on middle band suppressing orthogonal filter bank defined by low pass filter

$$h=[1/4, 2/4, 1/4];$$

– successively scaled orthogonal filtering (with low pass filter

$$h=[0.01995,-0.04271,-0.05224,0.29271,0.56458, 0.29271, -0.05224,-0.04271,0.01995]$$

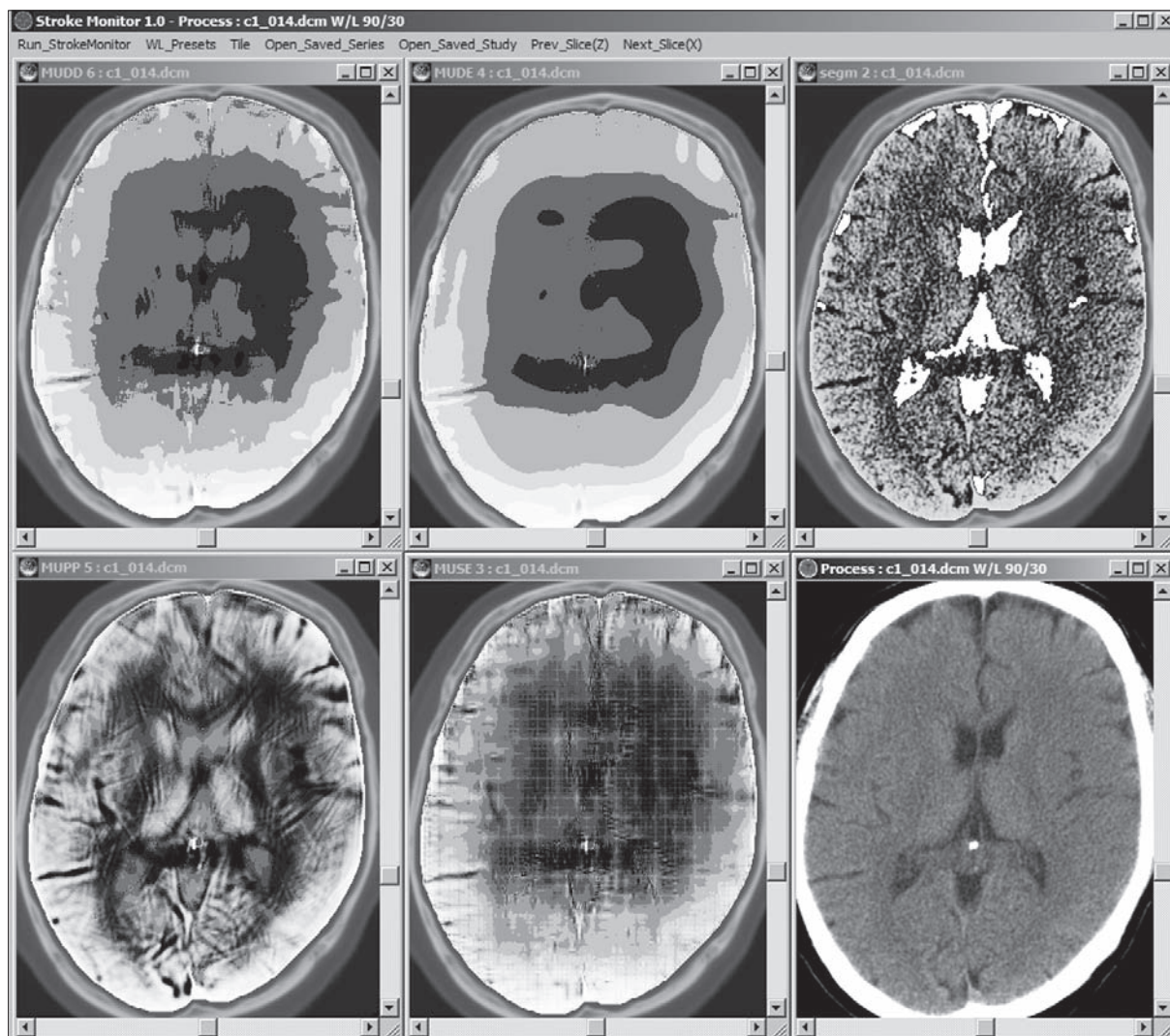


Figure 1. Interface of designed stroke monitor called MulCAS used for support of hyperacute stroke diagnosis. Four different forms of visual hypodensity expression was presented in two first image columns (up left – based on curvelet-wavelet kernels, up right – wavelet-curvelet basis, down left – only curvelet basis, down right – two wavelet basis). Down-right image is source scan data and top-right is its visualization after contrast equalization, with segmented and colored bright non-SSRs.

with adaptive soft thresholding in a set of middle-frequency subbands for increasing variability of lower density data. Moreover, simplified data visualization method that communicates enhanced pathology signs was used to make a distribution of brain tissue hypoattenuation more clear to the readers. The conclusions of experimentally evaluated efficiency of such diagnosis support reported in [11,26] are as follows: – the causes masking acute stroke symptoms may be significantly reduced by wavelet-based post-processing; – two-stage segmentation of the regions susceptible to ischemic density changes play dominant role in elimination of false diagnostic indications; – two-dimensional directional wavelet kernels, e.g. curvelets, are necessary to reconstruct smooth C^2 (twice continuously differentiable) region edges (tensor wavelet image decomposition represents contours as isolated edge points with a crucially large number of the expansion coefficients and the smooth edges are approximated inefficiently); – different forms of visualization adjusted to patient specificity and reader preferences are preferable. Therefore, new designed CAD tool was optimized according to these advices.

Multiscale computer-assistant of stroke diagnosis

Proposed method called multiscale computer-assistant of stroke (MulCAS) was based on nonlinear approximation of subtle hypodense signs as diagnostic content in multiscale domain. Such image content was approximated, extracted, enhanced and visualized in simplified forms of aiding 'magnifying glass'. In order to reveal unrecognized in routine assessment presence of tissue ischemia of cerebrum structures, and accurately confirm the brain damage through meaningful visual expression, the following algorithm was applied:

1. Initial stage of image conditioning with segmentation of stroke-susceptible regions (SSR) of brain tissues – locally adaptive region growing and thresholding methods and smooth complement of segmented diagnostic areas;
2. Essential stage of subtle hypodensity signs extraction in SSR by two subsequent multiscale decompositions giving four methods of processing:

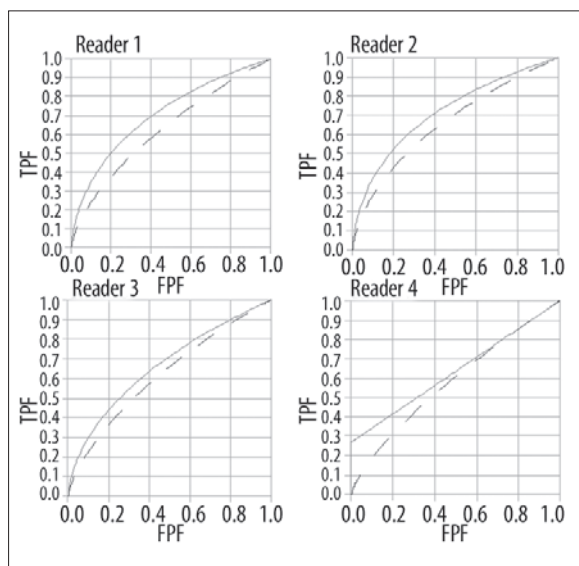


Figure 2. Detailed ROC curves of subsequent readers for acute stroke diagnosis according to test procedure. Dashed line is treatment I and solid line is treatment II (with MulCAS). Increased AUCs of MulCAS-supported diagnosis for each reader were noticed.

- a) target content estimation with tensor wavelet or curvelet basis as nonlinear approximants with adaptive semisoft thresholding;
- b) signal emphasizing with especially adjusted curvelet and tensor wavelet basis and additional thresholding controlled by semantic content models;
- 3. Final stage of visual hypodensity expression – display arrangement of processed SSR and source scans with greylevel quantization and contrast enhancement by dif-

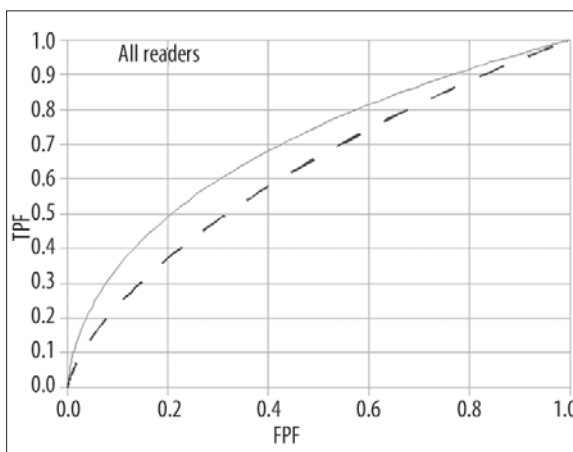


Figure 3. General ROC curves of all readers for acute stroke diagnosis according to test procedure. Dashed line is treatments I and solid line is treatment II (with MulCAS). Clearly increased AUC for MulCAS-supported diagnosis was noticed.

ferent forms of visualization, according to observer suggestions.

Computerized visual expression of hypodense signs with increased sensitivity to the subtle image manifestations of cerebral ischemia was constructed as additional view representing estimated diagnostic content with enhanced stroke symptoms synchronized to routine CT data preview (Figure 1).

Material and experimental procedures

Evaluation of test CT examinations was performed in 95 patients admitted to a hospital with symptoms suggest-

Table 1. Efficiency of acute stroke diagnosis for test readers participated treatments I (without MulCAS) and treatments II (with MulCAS).

Reader	AUC		Sensitivity		Specificity		Accuracy		PVP	
	I	II	I	II	I	II	I	II	I	II
1	0.612	0.658	0.381	0.426	0.789	0.800	0.463	0.505	0.879	0.889
2	0.580	0.612	0.436	0.526	0.789	0.789	0.505	0.578	0.892	0.909
3	0.585	0.638	0.526	0.763	0.631	0.631	0.547	0.736	0.851	0.892
4	0.546	0.638	0.197	0.276	0.894	1.000	0.336	0.421	0.882	1.000
Mean	0.580	0.636	0.384	0.498	0.776	0.805	0.463	0.560	0.876	0.923

Table 2. The results of DBM MRMC analysis for all readers, all test cases, and selected case subgroups with better quality, scanning or patient conditioning.

DBM MRMC analysis	AUC		p-value	
	I	II	CBM	TRAP
All test cases (95)	0.580	0.636	0.0000	0.0093
Cases without movement artifacts (85)	0.570	0.629	0.0000	0.0099
Cases without significant asymmetry (89)	0.627	0.675	0.0004	0.0146
Cases without scarring (59)	0.600	0.673	0.1502	0.0005

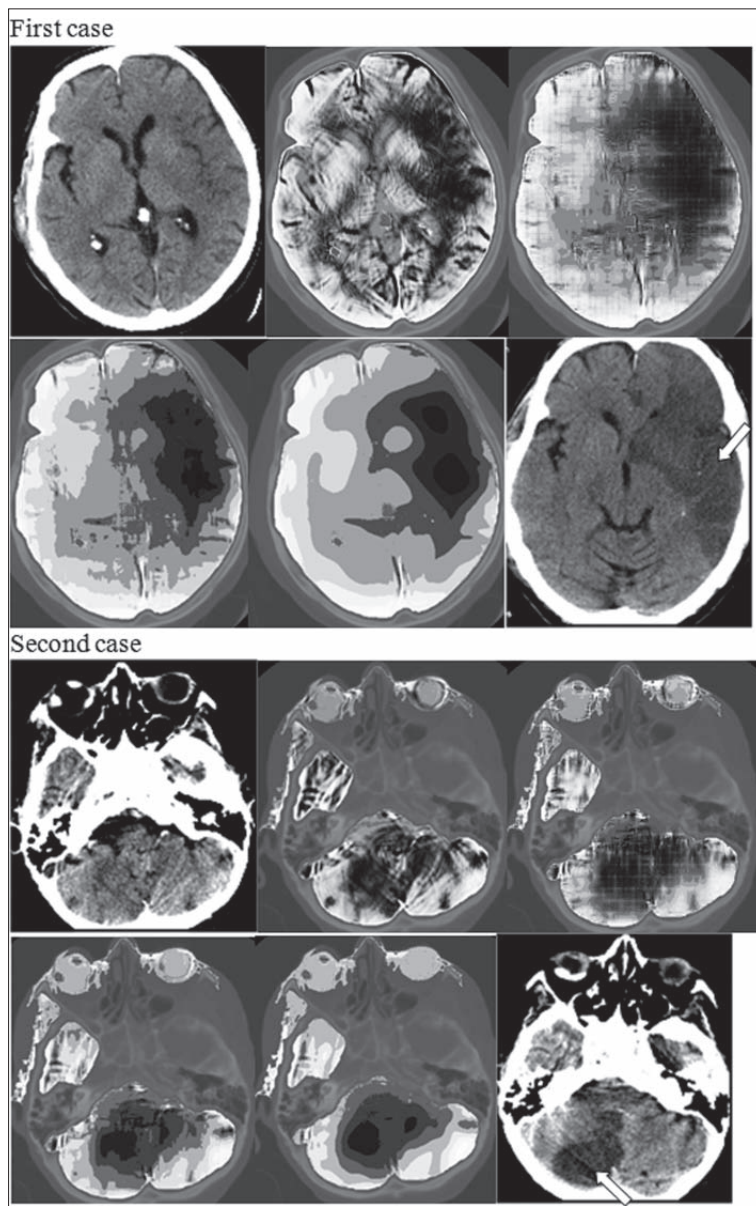


Figure 4. Two examples of hypoattenuation revealed by MulCAS with 4 form of extraction; for each case top-left is acute CT scan, top-middle: curvelets-based extraction, top-right: two wavelet-based extraction, down-left: curvelet and tensor wavelet-based extraction, down-middle: tensor wavelet and curvelet-based extraction; down-right: follow-up CT stroke confirmation with indicated areas of hypodensity.

ing stroke. The test set was selected by two neuroradiologists from our database of over 170 patients imaged with brain CT scans for stroke diagnosis. Criteria of choice of 76 patients aged 24–92 (mean 69.3 years) with proven infarction who underwent nonenhanced CT examinations of the head within first hours of stroke onset were diagnostic representativeness and interpretation difficulty because of hidden hypoattenuation. No direct hypodense signs of hyperacute ischemia were found on test data sets. Scans with unaccepted technical quality were excluded from consideration. The average time between the onset of symptoms and the CT examination was 4.48 hours. Additionally, 19 patients without infarction (with non-stroke changes) were chosen from this database as control patients. For that patients, stroke-like symptoms at the admission disappeared in the follow-up. The approximate 3.5:1 ratio of the number of study patients to the number of control patients more closely simulate our clinical experience. No cases with active bleeding, brain tumor nor contrast enhance-

ment were selected. Each test patient case consisted of around 22 regular CT scans synchronized in visualization to the same number of images obtained by designed CAD processing. Follow-up CT and/or DWI (from 1 to 10 days after the ictus) exam and/or clinical features confirmed or excluded the diagnosis of stroke constituting 'gold standard' to verify stroke detection performance.

Image review was performed independently at a diagnostic workstations of two radiological centers by four blinded neuroradiologists experienced in the interpretation of stroke CT images (treatments I). All test scans were subjectively rated by each reader according to the following relative 1–5 scale ("1" indicating definitely no possibility of stroke; "2" – a slight possibility of stroke; "3" – equivocal diagnosis; "4" – a greater possibility of stroke; "5" – a definite possibility of stroke) according to routine diagnostic procedure. For the rates 4 and 5 they were additionally asked to point out the location of ischemic focus. Formulated diag-

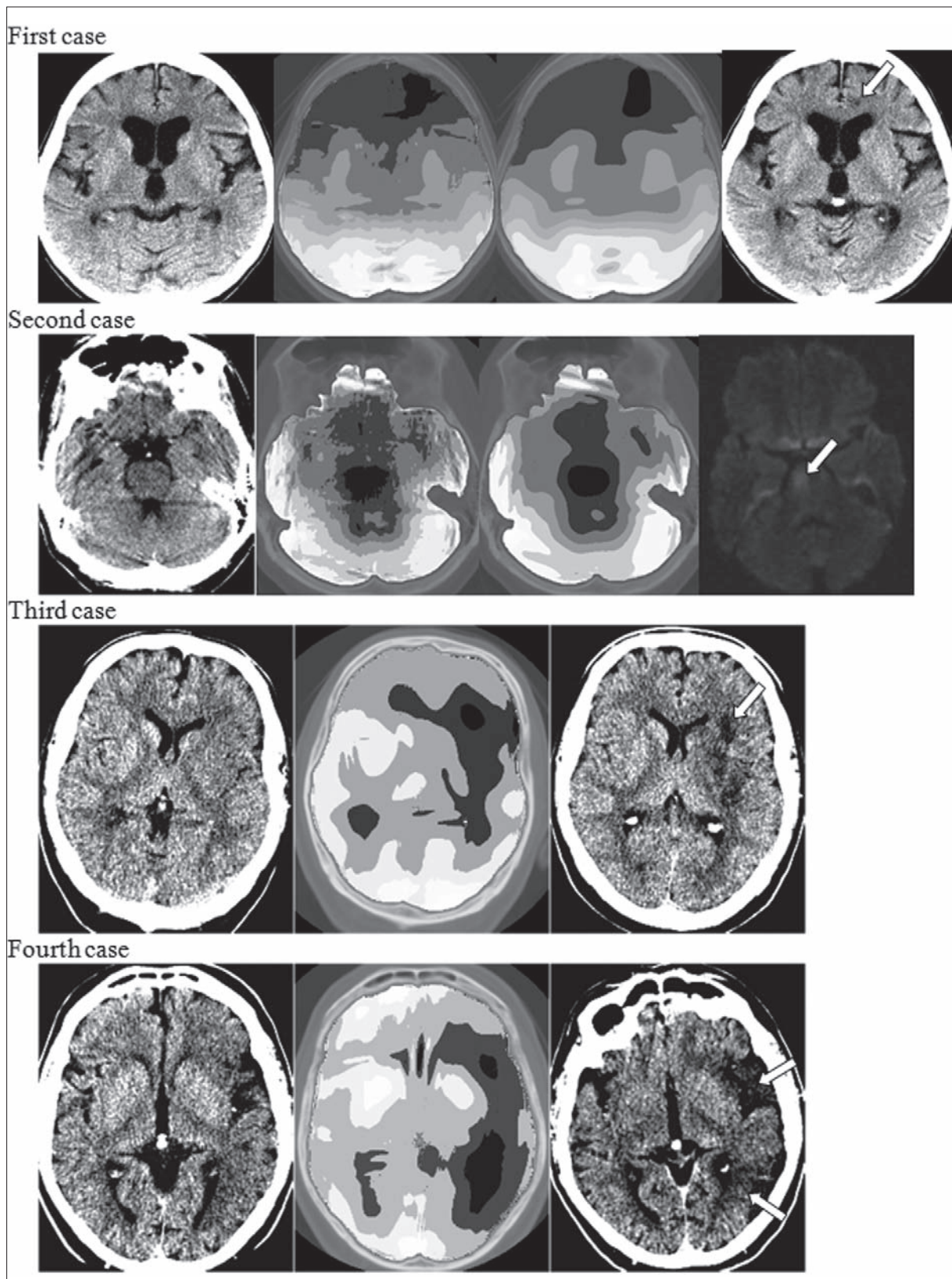


Figure 5. The examples difficult to reveal acute stroke CT cases with selected forms of CAD tool assistance; for each case left picture is acute CT scan, middle- map or maps of extracted hypodensity, right – follow-up CT or DWI (second case) stroke confirmation with indicated areas of hypodensity.

nostic scores could be changed in the next step of interpretation with additional aid of designed CAD tool (treatments II). Subjective rating of test scan was undertaken as previously according to the same 1–5 scale but taking into account additional preview of the scans processed by MulCAS synchronized to their source scans previewed according to routine preferences.

The statistical computations for paired test results were processed with software DBM MRMC 2.2 designed to perform an analysis of variance (ANOVA) when both reader and case variation are relevant to calculate the statistical significance of the differences between different treatments (diagnostic tests, or modalities). Statistical significance of difference between ROC indices when the performance of a diagnostic device is affected both by the cases analyzed (patient) and by the observer was determined.

Receiver operator characteristic (ROC) analyses were performed for test cases to evaluate the influence of MulCAS on radiological diagnosis. By comparing the areas under two ROC curves – for routine CT scan preview and additionally MulCAS-supported preview, a parametric and nonparametric approaches was applied and compared. DBM MRMC computed the ROC indices (first of all AUC) of the statistical analysis using contaminated binormal model (CBM) and empirical trapezoidal/Wilcoxon estimation (TRAP) without any distributional assumption. Moreover, other parameters characterizing reader detection efficiency were calculated to complete evaluation results.

Results

Statistic evaluation of the test results was based on reader performance combination with ROC-based analysis. The values of shape and area under curve (AUC), sensitivity, specificity, accuracy and PVP was estimated and compared for two test treatments: without CAD and with CAD and separately for each reader (Figure 2 and Table 1). Next, the impact of CAD tool on acute stroke diagnosis was monitored through values of AUC and p-value of significance level basing on general ROC curve estimation with CMB and TRAP data modeling (Table 2 and Figure 3). The examples of proposed computer assistance of acute stroke diagnosis were presented in Figure 4 and Figure 5.

Analysis of ROC curves indicates, that MulCAS as CAD tool had positive impact on detection of stroke for all radiologists participating experimental evaluation of diagnosis performance. The AUC values were clearly higher for CAD-supported CT scan interpretation. Verified hypothesis of ROC AUCs' equivalence for curves of treatments I and II was rejected because of p-values <0.05 what indicates sta-

tistically significant diagnosis performance improvement. Used material, test procedure and applied method of statistical analysis suggest more general usefulness of MulCAS in acute stroke diagnosis because of assumed analysis model of treating both readers and cases as random samples. Thus the evaluation results could be generalized to the population of readers and cases from which the used cases and readers were sampled.

The ROC curves and computed indices for all observers and all test cases illustrate the clinical situation, where the radiologist is supposed to evaluate every CT scan for existence or nonexistence of hyperacute ischemic changes regardless of image quality, patients age or clinical manifestation. Furthermore, detailed analysis for subsequent readers and subgroups of test cases confirms general tendency of diagnosis performance in selected test samples what supports reliability of computed, observed and concluded remarks. Thus, the general improvement of acute stroke diagnosis assisted with MulCAS was stated.

Conclusions

Routine CT completed with proposed method of computer assistance diagnosis provided noticeable better diagnosis efficiency of acute stroke according to the rates and opinions of all test readers. Proposed CAD tool for supporting acute stroke diagnosis gives additional expression maps for more sensitive visualization of brain tissue hypoattenuation in susceptible to ischemia territories. Diversified degrees of tissue density lowering were presented in subsequent forms basing on four algorithms of multiscale data representation and nonlinear approximation. Reported results indicate that combined evaluation of native CT together with hypodensity-oriented enhanced image may facilitate the interpretation of CT scans in hyperacute cerebral infarction.

According to conducted ratings and opinions, stroke display improved the diagnosis of early ischemic changes because of increased visibility and clarity of hypodense signs in test exam probe. Therefore, reliable display of hypodense signs can considerably accelerate the diagnosis of hyperacute ischemic stroke because of increased sensitivity. Planned optimization of MulCAS includes fully automatic detection of hypodense regions to complete assisted indications with the results of numerical characteristics of tissue features. The purpose are suggestions of acute stroke diagnosis formulated more objectively and explicitly. Planned prospective studies will let evaluate more accurately the impact of this CAD tool on diagnosis and further treatment in patients suffered from stroke. It is necessary to determine whether this method is possible to be applied widely.

References:

1. Chalela JA, Merino JG, Warach S: Update on stroke. *Curr Opin Neurol*, 2004; 17: 447–51
2. Adams H, Adams R, Del Zoppo G, Goldstein LB: Guidelines for the early management of patients with ischemic stroke, 2005 guidelines update, A scientific statement from the Stroke Council of the American Heart Association/American Stroke Association. *Stroke*, 2005; 36: 916–21
3. von Kummer R: The impact of CT on acute stroke treatment, in: P. Lyden (Ed.), *Thrombolytic Therapy for Stroke*. Humana Press, 2005; 249–78
4. Tomura N, Uemura K et al: Early CT finding in cerebral infarction. *Radiology*, 1988; 168: 463–67
5. von Kummer R, Allen KL et al: Acute stroke: usefulness of early CT findings before thrombolytic therapy. *Radiology*, 1997; 205: 327–33

6. Wardlaw JM, Mielke O: Early signs of brain infarction at CT: observer reliability and outcome after thrombolytic treatment – systematic review. *Radiology*, 2005; 235: 444–53
7. Osborn AG: *Diagnostic Neuroradiology*. Mosby, 1994
8. Doi K: Computer-aided diagnosis in medical imaging: Historical review, current status and future potential. *Comp Med Im Graph*, 2007; 31: 198–211
9. Giger ML: *Computer-aided diagnosis in medical imaging – A new era in image interpretation*. World Markets Research Centre, Tech Rep, 2000
10. Przelaskowski A: Computer-aided diagnosis: from image understanding to integrated assistance. *Advances in Soft Computing – Information Technologies in Biomedicine*, 2008; 47: 44–54
11. Sklinda K, Bargiel P, Przelaskowski A et al: Multiscale extraction of hypodensity in hyperacute stroke. *Med Sci Monit*, 2007; 13(Suppl.1): 5–10
12. Hoeffner EG, Case I, Jain R et al: Cerebral perfusion CT: technique and clinical applications. *Radiology*, 2004; 231: 632–44
13. Latchaw RE: Cerebral perfusion imaging in acutestroke. *J Vasc Interv Radiol*, 2004; 15: S29–46
14. Seidel G, Albers T et al: Perfusion harmonic imaging in acute middle cerebral artery infarction. *Ultrasound in Med & Biol*, 2003; 29(9): 1245–51
15. Tomura N, Uemura K, Inugami A et al: Early CT finding in cerebral infarction: obscuration of the lentiform nucleus. *Radiology*, 1988; 168: 463–67
16. Truwit CL, Barkovich AJ, Gean-Marton A et al: Loss of insular ribbon: another early CT sign of acute middle cerebral artery infarction. *Radiology*, 1990; 176: 801–6
17. Unger E, Littlefield J, Gado M: Water content and water structure in CT and MR signal changes: possible influence in detection of early stroke. *Am J Neuroradiol*, 1988; 9: 687–91
18. Dzialowski I, Weber J et al: Brain tissue water uptake after middle cerebral artery occlusion assessed with CT. *J Neuroimaging*, 2004; 14: 42–48
19. Bendszus M, Urbach H, Meyer B et al: Improved CT diagnosis of acute middle cerebral artery territory infarcts with density-difference analysis. *Neuroradiology*, 1997; 39(2): 127–31
20. Grimm C, Hochmuth A, Huppertz HJ: Voxel-based CT analysis for improved detection of early CT signs in cerebral infarction. *Eur Radiol*, 2005; B315
21. Hudyma E, Terlikowski G: Computer-aided detecting of early strokes and its evaluation on the base of CT images. *Proc IEEE Int Multiconf Comp Sci Inf Techn*, 2008; 251–54
22. Capobianco Guido R, Pereira JC: (guest editors): Wavelet-based algorithms for medical problems. Special issue of *Computers in Biology and Medicine*, 2007; 37(4)
23. DeVore RA: Nonlinear approximation. *Acta Numerica*, 1998; 7: 51–150
24. Hammond DK, Simoncelli EP: Nonlinear image representation via local multiscale orientation. *Courant Institute Technical Report*, 2005; 2005–75
25. Starck JL, Murtagh F, Candes EJ, Donoho DL: Gray and color image contrast enhancement by the curvelet transform. *IEEE Trans Image Proc*, 2003; 12(6): 706–17
26. Przelaskowski A, Sklinda K, Bargiel P et al: Improved early stroke detection: wavelet-based perception enhancement of computerized tomography exams. *Comp Biol Med*, 2007; 37: 524–33